Multi-channel nonlinearity compensation of PDM-QPSK signals in dispersion-managed transmission using dispersion-folded digital backward propagation

Cen Xia,[1,2,*] Xiang Liu,[1] S. Chandrasekhar,[1] N. K. Fontaine,[1] Likai Zhu,[2] and G. Li[2,3,4]

[1]*Bell Labs, Alcatel-Lucent, 791 Holmdel-Keyport Road, Holmdel, New Jersey 07733, USA*
[2]*CREOL-The College of Optics & Photonics, University of Central Florida, Orlando, Florida 32816, USA*
[3]*College of Precision Instrument and Opto-Electronic Engineering, Tianjin University, Tianjin, China*
[4]*li@creol.ucf.edu*
[*]*cxia@creol.ucf.edu*

Abstract: We demonstrate nonlinearity compensation of 37.5-GHz-spaced 128-Gb/s PDM-QPSK signals using dispersion-folded digital-backward-propagation and a spectrally-sliced receiver that simultaneously receives three WDM signals, showing mitigation of intra-channel and inter-channel nonlinear effects in a 2560-km dispersion-managed TWRS-fiber link. Intra-channel and adjacent inter-channel nonlinear compensation gains when WDM channels are fully populated in the C-band are estimated based on the GN-model.

OCIS codes: (060.1660) Coherent communications; (060.4370) Nonlinear optics, fibers.

References and links

1. X. Li, X. Chen, G. Goldfarb, E. Mateo, I. Kim, F. Yaman, and G. Li, "Electronic post-compensation of WDM transmission impairments using coherent detection and digital signal processing," Opt. Express **16**(2), 880–888 (2008).
2. E. Ip and J. M. Kahn, "Compensation of dispersion and nonlinear impairments using digital backpropagation," J. Lightwave Technol. **26**(20), 3416–3425 (2008).
3. L. Zhu and G. Li, "Folded digital backward propagation for dispersion-managed fiber-optic transmission," Opt. Express **19**(7), 5953–5959 (2011).
4. H. Louchet and A. Richter, "Characterization and mitigation of nonlinear impairments in multi-span transmissions using an equivalent single-span model," in *Proc. ECOC'11* (2011), paper We.10.P1.68.
5. L. Zhu and G. Li, "Nonlinearity compensation using dispersion-folded digital backward propagation," Opt. Express **20**(13), 14362–14370 (2012).
6. E. Ip, Y. K. Huang, E. Mateo, Y. Aono, Y. Yano, T. Tajima, and T. Wang, "Interchannel nonlinearity compensation for 3λ× 114-Gb/s DP-8QAM using three synchronized sampling scopes," in *Proc. OFC'12* (2012), paper OM3A.6.
7. N. K. Fontaine, X. Liu, S. Chandrasekhar, R. Ryf, S. Randel, P. Winzer, R. Delbue, P. Pupalaikis, and A. Sureka, "Fiber nonlinearity compensation by digital backpropagation of an entire 1.2-Tb/s superchannel using a full-field spectrally-sliced receiver," in *Proc. ECOC'13* (2013), paper Mo.3.D.5.
8. C. Xia, X. Liu, S. Chandrasekhar, N. K. Fontaine, L. Zhu, and G. Li, "Multi-channel nonlinearity compensation of 128-Gb/s PDM-QPSK signals in dispersion-managed transmission using dispersion-folded digital backward propagation," in *Proc. OFC'14* (2014), paper Tu3A.5.
9. A. Carena, V. Curri, G. Bosco, P. Poggiolini, and F. Forghieri, "Modeling of the impact of nonlinear propagation effects in uncompensated optical coherent transmission links," J. Lightwave Technol. **30**(10), 1524–1539 (2012).
10. R. Dar, M. Feder, A. Mecozzi, and M. Shtaif, "Properties of nonlinear noise in long, dispersion-uncompensated fiber links," Opt. Express **21**(22), 25685–25699 (2013).
11. X. Liu, A. R. Chraplyvy, P. J. Winzer, R. W. Tkach, and S. Chandrasekhar, "Phase-conjugated twin waves for communication beyond the Kerr nonlinearity limit," Nat. Photonics **7**(7), 560–568 (2013).
12. X. Liu, F. Buchali, and R. W. Tkach, "Improving the nonlinear tolerance of polarization-division-multiplexed CO-OFDM in long-haul fiber transmission," J. Lightwave Technol. **27**(16), 3632–3640 (2009).
13. C. Xie, "Suppression of inter-channel nonlinearities in WDM coherent PDM-QPSK systems using periodic-group-delay dispersion compensators," in *Proc. ECOC'09* (2009), P4.08.

#203705 - $15.00 USD Received 30 Dec 2013; revised 21 Feb 2014; accepted 23 Feb 2014; published 5 Mar 2014

14. X. Liu, S. Chandrasekhar, P. J. Winzer, B. Maheux-L, G.Brochu, and F. Trepanier, "Efficient fiber nonlinearity mitigation in 50-GHz-DWDM transmission of 256-Gb/s PDM-16QAM signals by folded digital-back-propagation and channelized FBG-DCMs," in *OFC'14* (2014), paper Tu3A.8.
15. E. F. Mateo, F. Yaman, and G. Li, "Efficient compensation of inter-channel nonlinear effects via digital backward propagation in WDM optical transmission," Opt. Express **18**(14), 15144–15154 (2010).

1. Introduction

Kerr nonlinearity in fiber imposes a fundamental limit on transmission capacity. Most of the already deployed long-haul fiber transmission systems are dispersion-managed (DM), which incur even more severe nonlinearity impairments as compared to dispersion-unmanaged systems. There are various methods for nonlinear compensation (NLC). One of the current strategies for nonlinear mitigation under intensive studies is digital backward propagation (DBP) [1,2]. However, this method is confronted with two major difficulties. One difficulty is its high digital signal processing (DSP) complexity. To reduce the computation complexity in long-haul DM systems, dispersion-folded DBP and its variations have been proposed [3, 4], and experimentally verified [5]. The other difficulty is its limited performance gain in wavelength-division multiplexed (WDM) systems. The performance gain was recently shown to be increased by multi-channel DBP in which multiple WDM channels are jointly processed to mitigate both intra-channel and inter-channel nonlinear effects [6, 7]. Recently, we demonstrated the use of multi-channel dispersion-folded DBP to realize NLC with increased performance gain and reduced DSP complexity in a Nyquist-WDM transmission system consisting of 37.5-GHz-spaced 128-Gb/s polarization-division-multiplexed (PDM) QPSK signals and a 2560-km dispersion-managed True-Wave-Reduced-Slope (TWRS) fiber link [8]. The dependences of the NLC performance on both receiver bandwidth and WDM signal bandwidth are also studied. Here, we present the experimental setups and results in more depth. Furthermore, we calculate the intra-channel and adjacent inter-channel nonlinear compensation when WDM channels are fully populated over C-band based on the GN-model. The calculated results show that intra-channel nonlinear compensation would no longer be very effective while adjacent inter-channel nonlinear compensation would offer only a small gain when the full C-band is populated.

2. Experimental setup

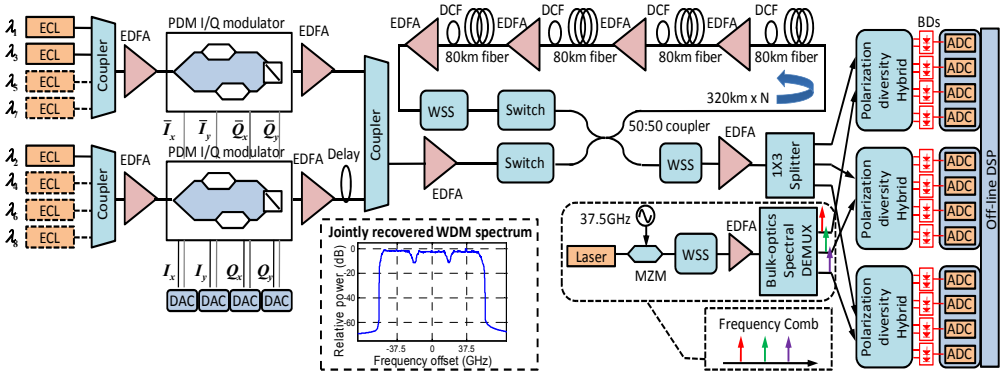

Fig. 1. Schematic of the experimental setup for multi-channel NLC with a spectrally-sliced coherent receiver and dispersion-folded DBP.

Figure 1 shows the experimental setup. To compare the performance with different aggregate WDM transmitter bandwidths, the Nyqusit-WDM transmitter is first composed of three and then of eight external cavity lasers centered near 1550 nm with a 37.5-GHz spacing. The lasers with linewidths of ~100kHz generate fine carriers, which are then divided into even and odd groups and separately modulated by two PDM I/Q modulators at 32 Gbaud. The drive signals for each modulator are from four digital-to-analog converters (DACs) operating at 2

#203705 - $15.00 USD Received 30 Dec 2013; revised 21 Feb 2014; accepted 23 Feb 2014; published 5 Mar 2014

samples per symbol or 64 GS/s. To obtain close channel spacing, a root raised-cosine (RRC) digital filter with a roll-off factor of 0.1 is applied to confine the optical spectrum of each signal. After the modulation, the even group is delayed for signal decorrelation and recombined with the odd group. The transmission link is a re-circulating loop comprising four spans of 80-km TWRS fiber, each followed by a dispersion-compensating fiber (DCF). The dispersion and Kerr nonlinear coefficient of the TWRS fiber are 4.66 ps/nm and 1.79 $W^{-1}km^{-1}$, respectively. The residual dispersion per span is about 36 ps/nm on average. Inline erbium-doped fiber amplifiers (EDFAs) are added after each span to compensate for the span loss. A wavelength selective switch (WSS) is used to reject out-of-band noise. The signals are propagated over 2560 km (32×80km) and only three center channels are detected by a spectrally-sliced receiver [7]. The receiver measures the signal spectrum slice by slice using a phase-locked and equally-spaced optical frequency comb, followed by stitching the slices digitally together to form a full-band electrical field. The lines of the frequency comb are precisely spaced by 37.5-GHz so that each line is able to serve as a local oscillator for coherent detection of the corresponding spectrum slice. Because the phase and amplitude is locked among the frequency comb lines, the received spectrum slices can be used to seamlessly reconstruct the full field of the three signals, and joint DSP can then be applied to realize multi-channel NLC. The frequency comb is generated by a Mach-Zehnder modulator (MZM) driven by an amplified 37.5-GHz sinusoidal wave to modulate an external cavity laser. The frequency comb is then equalized by a WSS and finally separated by a bulk-optics wavelength demultiplexer (DEMUX) including a fiber array, a collimating lens and a diffraction grating. To detect the spectrum slices, the WDM signals are split into three copies, each detected by a digital coherent receiver consisting of a polarization-diversity optical hybrid followed by four balanced detectors (BDs). The BD outputs are recorded by 40-GS/s analog-to-digital converters (ADCs), which also act as optical filters of 40-GHz cut-off bandwidth to slice the spectrum. Finally the signal spectrum (three channels only) is reconstructed, as shown in the inset of Fig. 1.

3. Folded-DBP v.s. conventional DBP

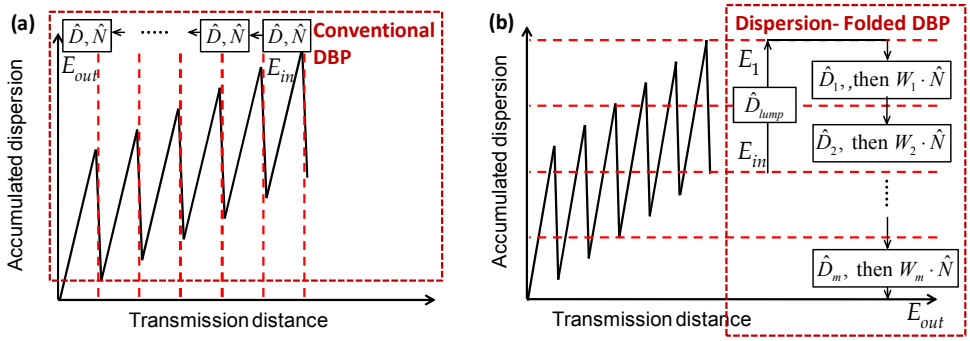

Fig. 2. Schemes of (a) conventional DBP and (b) dispersion-folded DBP.

The received signals are processed using a folded DBP algorithm and evaluated by the Q^2-factor, which is directly calculated from the measured bit-error ratio (BER) using $Q^2 = 20\log_{10}\left[\sqrt{2}\cdot erfcinv\left(2\cdot BER\right)\right]$. The conventional DBP uses the split-step fourier method to separately deal with dispersion and nonlinearity step by step in the reverse way of signal propagation along the fiber as Fig. 2(a) shows. The total step numbers thus determine the computation load. Folded DBP is trying to calculate steps with the similar dispersion and nonlinearity in one, i.e., fold the steps to save the large computation load. This becomes possible for a dispersion-managed system where the accumulated dispersion repeats often. Furthermore, it is found that the nonlinear distortions can be assumed the same too at

#203705 - $15.00 USD Received 30 Dec 2013; revised 21 Feb 2014; accepted 23 Feb 2014; published 5 Mar 2014

locations where the accumulated dispersion is identical. This is because that the waveform is dominated by the accumulated dispersion since the total nonlinear shift of the entire link at optimum power is rather small, on the order of 1 radian. Figure 2(b) shows the schematic of folded DBP, where the fiber segments with the same range of accumulated dispersion are folded into one step of DBP instead of being computed separately in conventional DBP. First, a lumped dispersion compensator ($\hat{D}_{lump}$) is applied to bring the received signal field E_{in} to the first folded DBP fiber segment E_1 . Then dispersion ($\hat{D}_i$ of i-th step) and nonlinear compensator ($\hat{N}_i$) are performed step by step with folded segments. Note that $W_i = \sum_k \gamma \int P_{i,k}(z)dz$ is a weighting factor effectively taking account of varied power levels $P_{i,k}(z)$ within each segment. The required steps for folded and conventional DBP to achieve maximum Q^2 at optimum signal launch power (P_{in}) are shown in Fig. 3(a) when 3 channels are transmitted, detected and processed. Folded DBP provides equal maximum gain as the conventional DBP, while saving the computation load by a factor of ~3.4 since the computation per step for both DBPs is similar. Figure 3(b) shows the performances of the two DBP schemes at a higher signal launch power (-2 dBm). Folded DBP saves the DSP load by a factor of 5 for a same Q^2 factor of 9.2 dB, giving a hint that folded DBP would save more when nonlinearity is larger. In addition, folded DBP algorithm has a potential to perform even better as a consequence of that more segments can be folded if residual dispersion per span is smaller or fiber dispersion is larger such as SSMF.

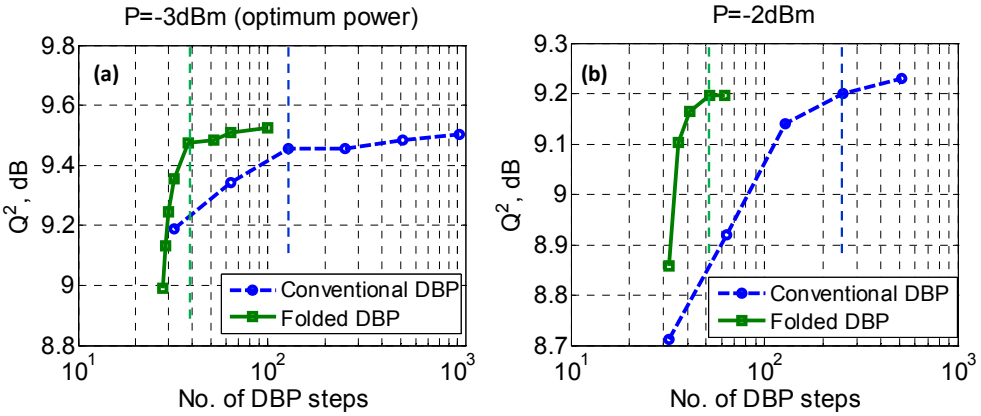

Fig. 3. Number of DBP steps needed in folded DBP compared to that needed in conventional-DBP at (a) Pin = –3 dBm (the optimum power) and (b) Pin = –2 dBm.

4. Experimental results

Figures 4 and 5 compare the signal quality of the center channel after DSP for two different cases: (1) three channels transmitted with a transmitted WDM signal bandwidth (B_{WDM}) of 112.5 GHz and (2) eight channels transmitted with B_{WDM} = 300 GHz. In both cases only three channels are received as the jointly recovered signal spectrum (the center three channels for the case of eight channels transmitted), which is enabled by the spectrally-sliced receiver. The recovered center channel is evaluated by Q^2-factor and displayed here with constellations. For each case, three compensation methods are used: (1) only electronic dispersion compensation (EDC); (2) only intra-channel nonlinear compensation using folded DBP, i.e., the effective receiver NLC bandwidth (B_{RX}) being 37.5 GHz; (3) inter-channel nonlinear compensation with the knowledge of adjacent channels using folded DBP, i.e., B_{RX} being 112.5 GHz. Method (2) is enabled by filtering the center channel digitally before compensation. Note that the performance of folded DBP is almost equal to that of conventional DBP, hence the results

#203705 - $15.00 USD Received 30 Dec 2013; revised 21 Feb 2014; accepted 23 Feb 2014; published 5 Mar 2014

of conventional DBP are not plotted here. With intra-channel NLC, the highest achievable Q^2 improvement compared to EDC only, i.e., NLC gain, is 1.0 dB when three channels are transmitted (B_{WDM} = 112.5 GHz) and 0.6 dB when eight channels are transmitted (B_{WDM} = 300 GHz). Furthermore, the use of inter-channel NLC with the knowledge of two adjacent channels (B_{RX} = 112.5 GHz) gives 2.0 dB and 1.1 dB NLC gains respectively for these two cases. These results suggest that multi-channel NLC provides substantial performance gain over the intra-channel NLC by additionally mitigating inter-channel nonlinear impairments, especially when B_{RX} is the same as B_{WDM}. When B_{WDM} becomes larger than B_{RX}, the inter-channel nonlinear impairments resulting from the WDM channels outside the receiver detection/processing bandwidth cannot be compensated digitally, which decreases the effectiveness of DBP.

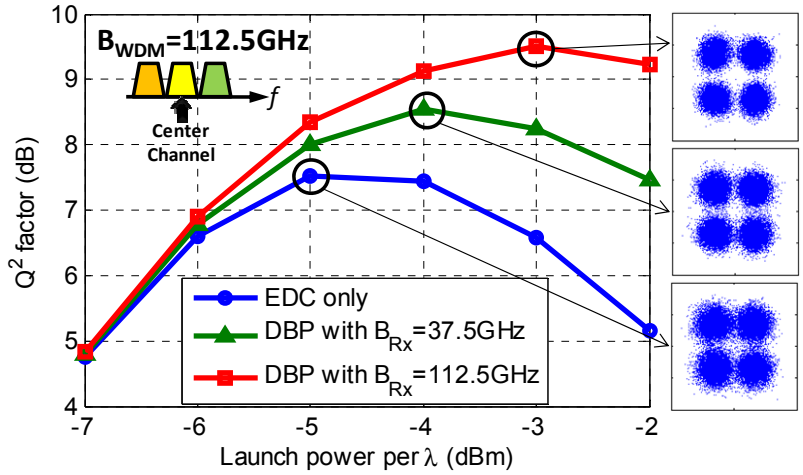

Fig. 4. Measured signal quality as a function of signal launch power per channel for the cases of 3 channels transmitted.

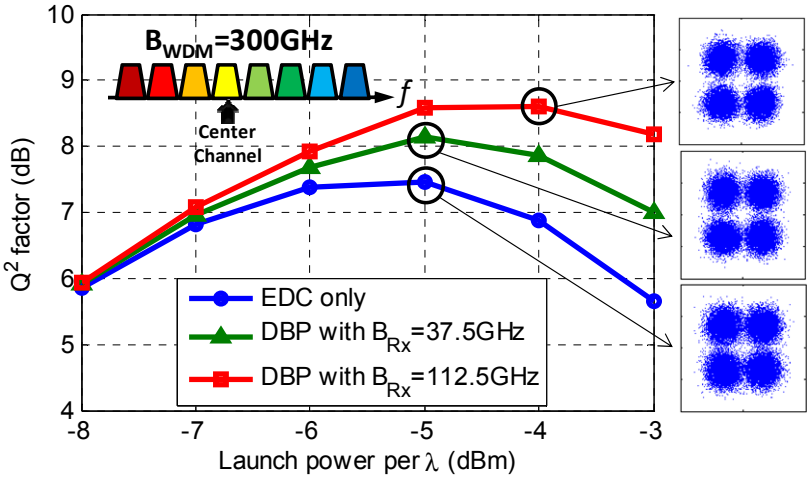

Fig. 5. Measured signal quality as a function of signal launch power per channel for the cases of 8 channels transmitted.

5. Scaling rules of intra-channel and inter-channel nonlinear compensation

The experiment above demonstrate NLC for the cases when three (B_{WDM} = 112.5GHz) and eight (B_{WDM} = 300GHz) WDM channels are transmitted. However, practical WDM system

#203705 - $15.00 USD Received 30 Dec 2013; revised 21 Feb 2014; accepted 23 Feb 2014; published 5 Mar 2014

channel count is around 100 in which the entire C-band is fully populated. To estimate the effectiveness of intra-channel and adjacent inter-channel NLC described above for the full C-band WDM system,, we modeled the nonlinear noise power (σ_{NL}^2) as a function of receiver bandwidth, using the Gaussian noise (GN) model [9] in which it was shown that the nonlinear noise can be treated as additive Gaussian noise. Although the GN model is proposed for dispersion-unmanaged systems, it is expected to also work reasonably well for long-distance dispersion-compensated transmission with high-speed modulation and sufficiently large residual dispersion per span (RDPS). To verify the validity of GN model for our DM system, the probability density functions of the noise in one of polarizations after 2560km propagation and dispersion compensation are plotted in Fig. 6 for a transmitted WDM signal bandwidth (B_{WDM}) of (a) 112.5 GHz and (b) 300 GHz at high power levels. As shown in the figure, the PDFs can be fitted well into a Gaussian function. Under the GN model, the power spectral density of the nonlinear noise in the dispersion-unmanaged system can be evaluated by one integral equation related to basic system parameters as below,

$$G_{NLI}(f)=\frac{16}{27}\gamma^2 L_{eff}^2\cdot\int_{-\infty}^{+\infty}\int_{-\infty}^{+\infty}G_{WDM}(f_1)G_{WDM}(f_1)G_{WDM}(f_1)\cdot\rho(f_1,f_2,f)\cdot\chi(f_1,f_2,f)df_2df_1, \quad (1)$$

where terms and symbols with detailed explanations can be found in ref [8]; one term needs to be emphasized is the phase-array factor $\chi(f_1,f_2,f)=\dfrac{\sin^2\left[2N_s\pi^2(f_1-f)(f_2-f)\beta_2L_s\right]}{\sin^2\left[2\pi^2(f_1-f)(f_2-f)\beta_2L_s\right]}$, which accounts for coherent interference effects of nonlinear noise in each span. One can use Eq. (1) to integrate over the wanted frequency band and thus is able to give bandwidth dependence. For the modeling of the dispersion-managed case, $\beta_2L_s=RDPS\cdot\lambda^2/2\pi c$ is substituted into the phase-array factor instead of using $\beta_2L_s=|D|L_s\cdot\lambda^2/2\pi c$ as for dispersion-unmanaged case.

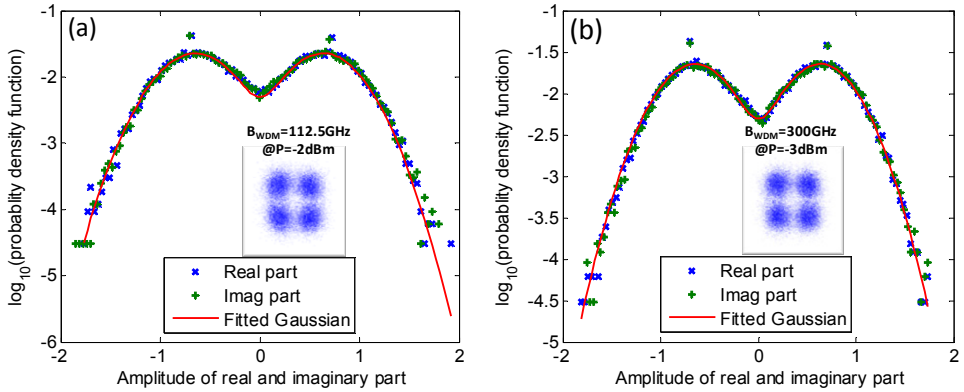

Fig. 6. Probability density functions (PDFs) of real and imaginary components of noise in one of the polarizations as well as fitted Gaussian distribution for (a) B_{WDM} = 112.5 GHz at the launch power of −2dBm per λ and (b) B_{WDM} = 300 GHz at the launch power of −3dBm per λ.

In what follows, the effective bandwidth B_{RX} is represented by n, the number of channels detected/processed. The total number of WDM channels is N. Figure 7 plots the normalized σ_{NL}^2 v.s. B_{RX} using SSMF and TWRS fibers as a comparison for both dispersion-unmanaged (DUM) and -managed (DM) cases with different RDPS for otherwise the same parameters as

#203705 - $15.00 USD Received 30 Dec 2013; revised 21 Feb 2014; accepted 23 Feb 2014; published 5 Mar 2014

the above experiment. All the NL noise power σ_{NL}^2 is normalized by the NL noise power in the SSMF DM case with 100 channels. The nonlinear Kerr coefficients used for SSMF and TWRS fibers are 1.3 $W^{-1}km^{-1}$ and 1.79 $W^{-1}km^{-1}$ respectively while the fiber dispersion parameters for SSMF and TWRS fibers are 16.5 ps/nm/km and 4.65 ps/nm/km. By simply comparing Figs. 7(a) and 7(b), one can conclude that SSMF performs better than TWRS not only for the DUM case, but also for the DM case when the same values of RDPS are used. For SSMF system alone, the NL noise power reduces more at larger RDPS, slowly approaching the performance of DUM case; while for TWRS system, the trend is similar to SSMF but the impact of RDPS is even stronger due to smaller fiber dispersion. Because of the above findings, for NLC with limited receiver bandwidth B_{RX} as usually $B_{RX} \le 3$, the gain is typically larger when the fiber dispersion is larger or when RDPS is larger.

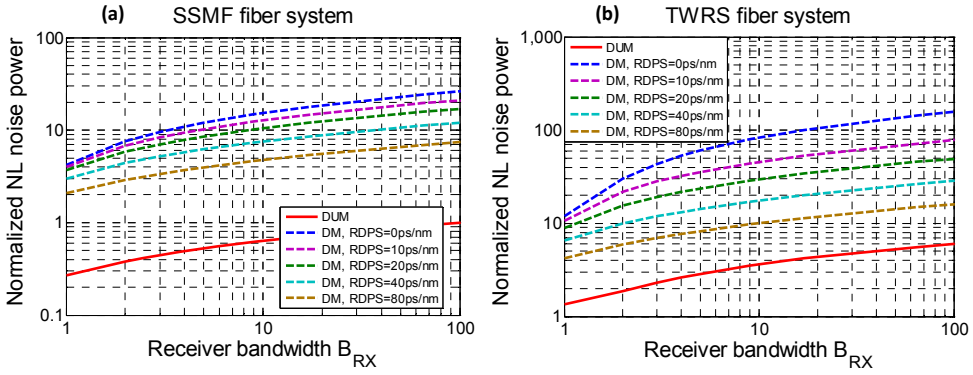

Fig. 7. Normalized nonlinear noise power versus the effective receiver NLC bandwidth (in units of channel bandwidth) for both DUM transmission and DM transmission with different RDPS values in links using (a) SSMF spans and (b) TWRS spans. DM: dispersion-managed; DUM: dispersion-unmanaged.

To give a detailed analysis for NLC gain, if a nonlinear compensation ratio $a_{NLC}(B_{RX}=n)$ is assumed as the result of using DBP with a receiver bandwidth of n channels, the NLC gain can be represented by,

$$\Delta Q^2 = \frac{1}{3}.10\log_{10}\frac{\sigma_{NL}^2(B_{RX}=N)}{\sigma_{NL}^2(B_{RX}=N)-a_{NLC}(B_{RX}=n)\cdot\sigma_{NL}^2(B_{RX}=n)}. \quad (2)$$

Accordingly, the larger the portion of σ_{NL}^2 within the effective NLC bandwidth B_{RX}, the larger the NLC gain. Figure 8 shows the normalized σ_{NL}^2 as a function of B_{RX} three cases of N = 3, 8, and 100 for current DM experiment using TWRS spans with a RDPS of 36 ps/nm. The corresponding NLC gains calculated according to Eq. (1) are marked on the figure by the triangular and star markers for intra-channel ($B_{RX}=1$) and adjacent inter-channel DBP ($B_{RX}=3$) respectively. Taking the intra-channel DBP for example, the detailed calculation is as follows. First, intra-channel NLC ratio $a_{NLC}(B_{RX}=1)$ is estimated to be 93% given the experimentally demonstrated 1 dB NLC gain for N = 3, indicated by the top blue triangular markers. Then the NLC gain for N = 8 and 100 can be calculated as 0.64 dB and 0.33 dB using $a_{NLC}(B_{RX}=1)$ = 93%. Similarly for adjacent inter-channel DBP as the purple star markers show, $a_{NLC}(B_{RX}=3)$ is estimated to be 75%, given the experimentally

#203705 - $15.00 USD Received 30 Dec 2013; revised 21 Feb 2014; accepted 23 Feb 2014; published 5 Mar 2014

demonstrated adjacent inter-channel NLC gain for N = 3. Then the adjacent inter-channel NLC gain for cases of N = 8 and 100 can be estimated as 1.1 dB and 0.54 dB. The estimated NLC gain of 0.64 dB and 1.1 dB for N = 8 using intra- and inter-channel NLC are very close to the experimental results of 0.69 dB and 1.0 dB. In the meantime, the results for N = 100 suggest that intra-channel nonlinear compensation would no longer be very effective when WDM channels are fully populated over the C-band. Even adjacent inter-channel NLC only yields a small NLC gain. Note that recent models that take into consideration signal modulation format and dispersion mapping [10,11] could be used to obtain more accurate estimation on the dependence of the NLC gain on the effective NLC bandwidth.

To increase the gain of NLC in the presence of many WDM channels, two approaches can be considered. First, optical inter-channel nonlinearity mitigation scheme based on periodic-group-delay dispersion-compensation [12–14] can be employed to suppress the nonlinear interactions from other WDM channels. Second, the inter-channel NLC bandwidth can be increased to include more neighboring channels using either full-field compensation or selective nonlinearity compensation that does not require phase locking in detecting WDM channels [15].

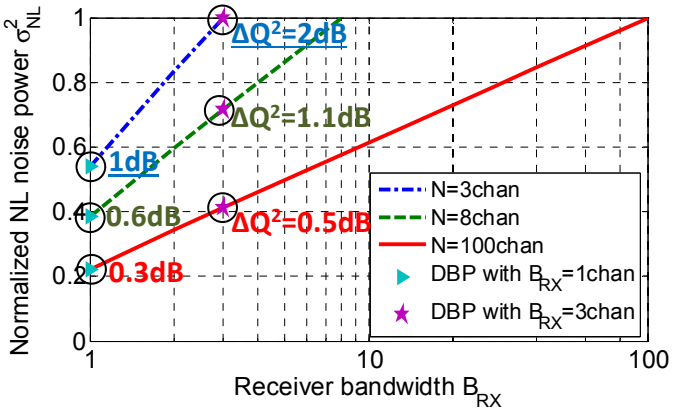

Fig. 8. Normalized nonlinear noise power v.s. the effective receiver bandwidth as channel numbers at the cases of 3, 8, 100 transmitter channels for current dispersion-managed system. The markers show intra-channel and adjacent inter-channel NLC using DBP: the underlined blue annotations represent experimental gains ΔQ^2 and other annotations in green and red represent estimated results. B_{RX}: the number of the receiver channels; N: the number of the transmitter channels.

6. Conclusions

We have experimentally demonstrated multi-channel nonlinear compensation using dispersion-folded DBP in a spectrally-sliced receiver for Nyquist-WDM transmission of 37.5-GHz-spaced 32-Gbaud PDM-QPSK signals over a 2560-km dispersion-managed TWRS fiber link. Combined with dispersion-folded DBP, the multi-channel NLC provides additional performance gain over the single-channel NLC, as well as reduced DSP complexity as compared to the conventional DBP. The dependences of the intra-channel and inter-channel nonlinear compensation gains on the number of WDM channels and the NLC bandwidth are estimated by using the GN-model. Potential approaches to further increase the NLC gains in dispersion-managed DWDM systems are also briefly discussed.

Acknowledgments

The authors wish to thank Dr. P. J. Winzer for support. This research was supported in part by the National Basic Research Programme of China (973) Project #2014CB340100.

#203705 - $15.00 USD Received 30 Dec 2013; revised 21 Feb 2014; accepted 23 Feb 2014; published 5 Mar 2014